JOURNAL OF MATERIALS SCIENCE 21 (1986) 3491–3496

Effects of annealing on the grain boundary potential barrier of ZnO varistor

EUN DONG KIM, MYUNG HWAN OH, CHONG HEE KIM
Korea Advanced Institute of Science and Technology, PO Box 131, Cheongryang, Seoul, Korea

Effects of post heat treatment on the potential barrier at the grain boundaries of ZnO varistors will be discussed from the viewpoints of the surface state density and the donor concentration. Leakage current of varistors at a low electric field increases by annealing at 750° C in air or nitrogen due to the lowered barrier height corresponding to the decrease of surface state density, which may be explained with the phase transformation of the bismuth-rich intergranular layer. It is also observed that the *V–I* non-linearity of the annealed ceramics is generally recovered as the annealing (in air) time is extended. This can be explained by the heightened barrier potential attributed to the decrease of donor concentration in ZnO grains, which was confirmed by aid of *C–V* measurements. The decrease of donor concentration by the annealing in air can be considered to be responsible for the thermal oxidation of interstitial zinc ions or oxygen vacancies.

1. Introduction

ZnO based ceramics with additional metal oxides such as Bi_2O_3, Sb_2O_3, CoO, MnO and Cr_2O_3 show highly non-ohmic voltage (V)–current (I) characteristics [1].

It has been generally accepted that the non-linear $V–I$ characteristics are strongly attributed to their microstructure composed of n-type semiconducting ZnO grains and intergranular layer [2–5].

The typical $V–I$ relationships of ZnO varistors can be generally divided by three behaviour zones.

At low current region, so called leakage current or prebreakdown region, the $V–I$ characteristic is explained by the thermally-activated conduction over the potential barriers formed at the grain boundaries [4–6].

In the varistor action region with high non-linearity (breakdown region), the highly non-ohmic relationship between applied electric field and conduction current can be expressed by the following empirical equation,

$$J = KE^{\alpha} \qquad (1)$$

where J is the current density ($A\,cm^{-2}$), E the externally applied electric field ($V\,cm^{-1}$), α the non-linear exponent (non-linearity), and K a constant related to the varistor. The non-linear exponent can be obtained by

$$\alpha = \frac{\log (J_1/J_2)}{\log (E_1/E_2)} \qquad (2)$$

where E_1 and E_2 are the electric fields applied between two electrodes when the current flow densities through the varistor are J_1 and J_2, respectively. It is generally regarded that the high non-linearity in this region arises from the tunnelling of carriers through the boundary barrier [4, 7, 8].

At high current region, so-called "upturn region", the conduction current is limited by the intrinsic resistivity of ZnO grains [9].

In the early papers with regard to the annealing effects in ZnO varistors, it was reported that degraded $V–I$ characteristics due to an electrical overstress could be restored by heat treatment at about 350° C [10, 11]. Iga and co-workers [12] have reported that ZnO ceramics annealed at 750° C in air show less current creep. It has been also observed that the heat treatment causes phase transformations and morphological changes of bismuth-rich intergranular layer [12, 13].

Inada [13] has reported that the non-linearity in $V–I$ relationships decreases abruptly by annealing at 700 to 800° C, which may be corresponding to the phase transformations of the intergranular layers and the formation of an unknown crystalline phase (cubic structure). It has been also observed that the varistor non-linearity is recovered by heat treating in air at 900 to 1100° C, probably attributed to phase transformations of the layers to their initial states before the treatment.

It was already known that the heat treatment on ZnO powders causes the phenomenon that interstitial zincs (Zn_i) diffuse out and combine with oxygens to form new lattices of ZnO at the surfaces [14].

Eda *et al.* [15] have proposed that both the phase transformations of intergranular layers and the oxidation of the donor defects are responsible for the improvement of stability of ZnO varistors under electrical stress.

But the origin of the decrease in the varistor non-linearity is not yet explained from the viewpoint of conduction mechanism [16]. In this paper, the effects of annealing on the $E–J$ characteristics will be discussed in terms of surface state density and donor concentration, which determine the barrier voltage at the grain boundaries in ZnO varistors.

0022–2461/86 $03.00 + .12 © *1986 Chapman and Hall Ltd.*

TABLE I Effects of annealing time (in air) on the non-linear exponent α, the leakage current J_l, and the power consumption P_l of the Co_2O_3-doped ZnO varistors (sintering condition; 1150° C in air for 1.5 h, annealing condition; 750° C in air).

Samples		α*	J_l‡ ($0.5F_0$†) ($A\,cm^{-2}$)	P_l§ ($0.5F_0$) ($W\,cm^{-3}$)
As-sintered		33.0	1.5×10^{-8}	1.05×10^{-5}
Annealed	0.4 h	3.3	4.0×10^{-5}	1.72×10^{-2}
	1.0 h	5.0	1.5×10^{-5}	0.64×10^{-2}
	3.0 h	6.3	8.0×10^{-6}	0.43×10^{-2}

*α: the non-linear exponent measured from 1 $\mu A\,cm^{-2}$ to 1 $mA\,cm^{-2}$.
†F_0: the varistor-operating electric field at the current density of 1 $mA\,cm^{-2}$.
‡J_l ($0.5F_0$); the varistor leakage current at $F = 1/2F_0$.
§P_l ($0.5F_0$); the power consumption at $F = 1/2F_0$.

2. Experimental details

2.1. Sample preparation

The non-ohmic ZnO varistors were prepared by the conventional ceramic fabrication procedure.

Guaranteed reagent grade raw materials of 99.0 ZnO–1.0 Bi_2O_3 and 98.5 ZnO–1.0 Bi_2O_3–0.5 Co_2O_3 (mol %) were mixed by wet-milling and then dried. After calcining at 750° C for 1 h, the calcined powders were ground by a agate mortar for 2 h and then pressed under a pressure of 500 $kg\,cm^{-2}$. Pressed discs were sintered at 1150° C in air for 1.5 h. Some of the sintered ceramics were annealed at 750° C in air, argon, or nitrogen atmosphere for various times. After lapping both faces of the varistor samples to ensure parallel and plane, silver paste (Dotite D-550, Hujisho, Japan) was applied on the faces.

2.2. Measurements of electrical properties

The V–I characteristics of varistor samples were measured by use of regulated d.c. power supplies up to a current range of 1 mA and in higher current region, by aid of surge current generators with built-in storage oscilloscopes, respectively.

The capacitance (C)–voltage (V) characteristics were determined at 1 kHz with a capacitance bridge having a bias voltage range from 0 to 100 V.

2.3. Analyses of microstructure and crystalline phases.

Crystalline phases of the ceramics were identified by the X-ray powder diffraction method. The powders for this were prepared by leaching the sample with 10 N NaOH for 10 h in order to detect small amounts of Bi_2O_3.

For electron microscopic analysis, the fractured surfaces of specimens were polished and etched with 5 N NaOH for 10 min.

3. Results and discussion

The applied electric field (E)–flowing current density (J) characteristics of the ternary system sample annealed in air at 750° C for 1 h were compared with that of the as-sintered in Fig. 1.

From Fig. 1, it can be easily seen that the current density at a low electric field (leakage current, defined in Table I) is dramatically increasing by the treatment, commensurate with the decrease of non-linear exponent α (defined in Table I). This result is in good agreement with the previous reports [13, 17].

The leakage current J_l at a constant low electric field can be described by

$$J_l = J_0 \exp(-q\Phi/kT) \quad (3)$$

where q is the electron charge, k the Boltzmann constant, T the ambient temperature (K), J_0 the constant related to E and T, and Φ the barrier voltage at a grain boundary.

From Fig. 1 and Equation 3, it may be considered that the barrier potential is lowered by annealing at 750° C in air.

The potential barrier Φ can be written as follows

$$\Phi = \varnothing - \xi \quad (4)$$

where $\varnothing$ is the built-in voltage which means the voltage difference between the bottom level of the conduction band of ZnO and the peak level of the band-bending at the grain boundary, and ξ is the difference between the Fermi level and the bottom of the conduction band of ZnO, which is expressed as,

$$\xi = (kT/q)\ln(N_c/N_d) \quad (5)$$

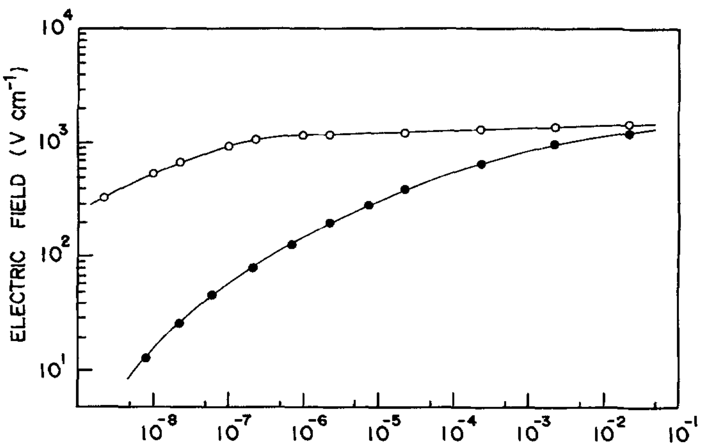

Figure 1 Effect of annealing on the E–J characteristics of Co_2O_3-doped ZnO varistor. (○) before RT, (●) after RT in air; at 750° C for 1 h.

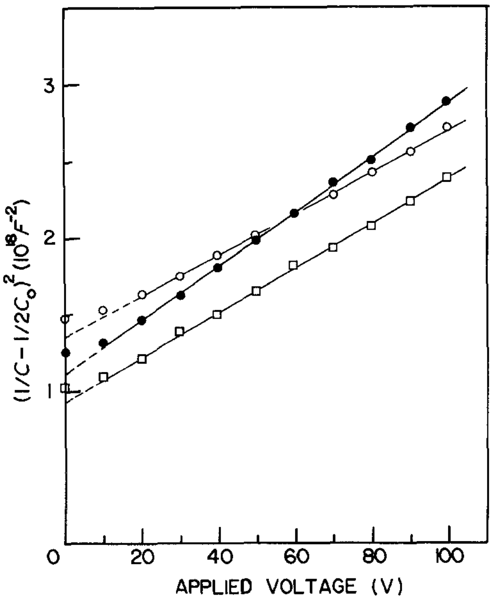

Figure 2 Capacitance–voltage characteristics of (99.0) ZnO–(1.0) Bi_2O_3 composite after treated at 750° C in different atmospheres. Electrode area = 0.45 cm^2; thickness 1.3 mm. (○) before RT, (●) after RT in air, (□) after RT in argon; at 750° C for 1 h.

where N_c and N_d are the number of energy state in the conduction band and the donor density of ZnO, respectively.

$\varnothing$ can be described in terms of the surface state density N_s at the interface of grain boundaries, as written in Equation 6 [18]

$$\varnothing = qN_s^2/2\varepsilon_s N_d \qquad (6)$$

where ε_s is the dielectric constant of ZnO.

According to Equations 3 to 6, it can be seen that the grain boundary potential Φ becomes a function of N_s and N_d.

$\varnothing$ and N_s have been experimentally obtained from C–V characteristics [6, 9, 19]. The voltage dependence of electrostatic capacitance in ZnO ceramic varistors can be approximated as follows [20]

$$(1/C - 1/2C_0)^2 = 2(\varnothing + V)/q\varepsilon_s N_d \qquad (7)$$

$$1/C_0 = 2(\varnothing/q\varepsilon_s N_d)^{1/2} \qquad (8)$$

where C_0 and C are the capacitance per unit area of a grain boundary without and with bias, respectively, and V the applied voltage per grain boundary.

Fig. 2 shows the relationships between $(1/C - 1/2C_0)^2$ and V for ZnO–Bi_2O_3 binary composites before and after annealing at 750° C in air or argon. It is noted that the effects for the ternary system varistors were similar to the case of binary system samples, shown in Fig. 2.

$\varnothing$ can be determined from the intersection of the extrapolated line of the plot with the voltage axis, while N_d can be calculated from the slope of the plot, if the number of boundary junctions within current-flowing paths in the varistor were known. Since it is unlikely that the average grain size of ZnO varies during the post treatment, the relative magnitude of N_d and $\varnothing$ can be derived from Fig. 2, although the exact number of grain junctions is not countable. As Fig. 2 shows no evidence such that the donor concentration is increasing, it can be believed that the decrease of Φ is mainly corresponding to the decrease of $\varnothing$, regardless of annealing atmosphere. This means that the abrupt decrease of $\varnothing$ by annealing at 750° C is not attributed to reduction or oxidation processes but corresponding to critical phenomena such as phase transformation. Iga [12] and Inada [13] have reported that crystalline phase of Bi_2O_3-rich intergranular layer are transformed from β- and δ-phase to γ-phase and the morphology of the layer be changed to a coarse state by heat treating at 700 to 800° C (in multicomponent systems).

In this study, the morphological change of intergranular layer was examined as shown in Fig. 3.

Fig. 4 shows that in all cases of as-sintered samples, the crystalline phase of Bi_2O_3 layers turned out to be α-phase (monoclinic) as in case of ZnO–Bi_2O_3 composite [21]. However, the α-phase of Bi_2O_3 was transformed to γ-phase after annealing at 750° C in air or inert atmosphere, which can be seen in Fig. 4.

From these observations and the previous reports

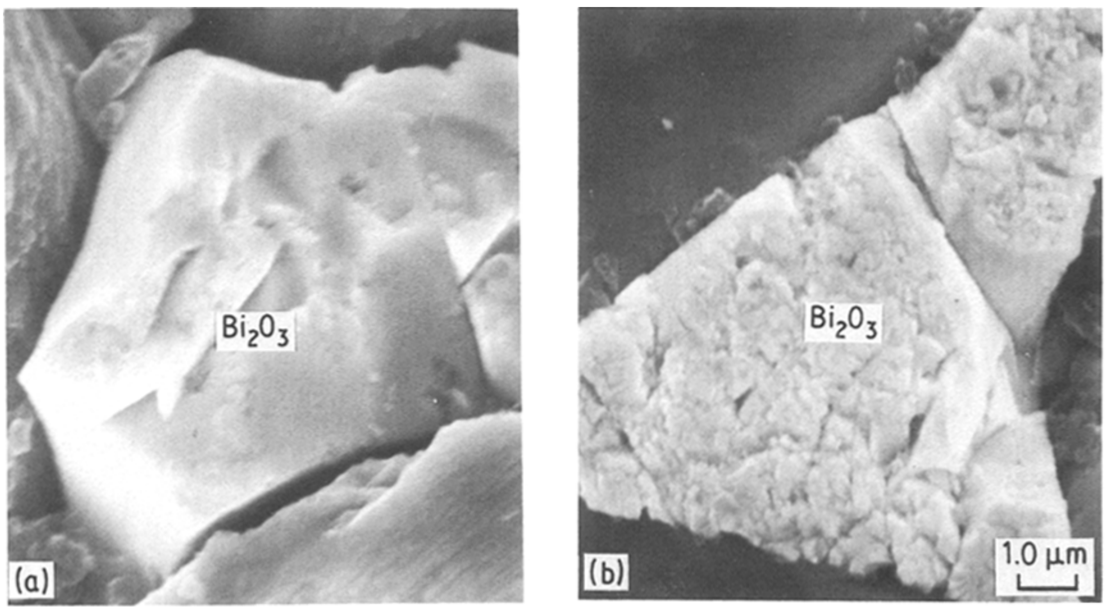

Figure 3 Scanning electron micrographs of Co_2O_3-doped ZnO ceramic (a) before and (b) after reheat-treated at 750° C for 1 h in air.

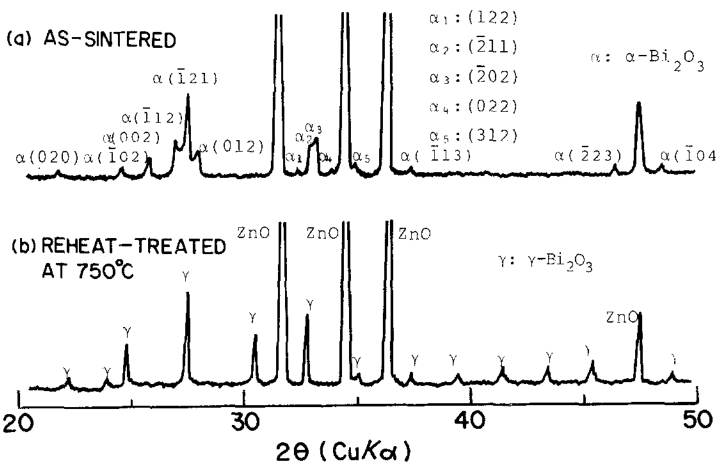

Figure 4 X-ray diffraction patterns (Cu$K\alpha$) of Co_2O_3-doped ZnO varistor (a) before and (b) after reheat-treated.

[12–17], it may be concluded that the lowering of built-in voltage $\varnothing$ by annealing process is attributed to smaller value of N_s, corresponding to the phase transformation of bismuth-rich intergranular layer.

If N_d were decreased at a constant N_s, not only $\varnothing$ but also ξ should be increased, which, in turn, should result in a higher barrier height, according to Equations 4 to 6. We could have already observed from Fig. 2 that N_d is considerably decreased by annealing in air but hardly influenced by annealing in argon atmosphere. Therefore it can be easily conscious that an oxidation atmosphere during annealing elevates the barrier height level in comparison with the effect of inert gases such as argon and nitrogen.

Meanwhile, Fig. 5 shows the effect of atmosphere during annealing on the *E–J* characteristics of Co_2O_3-doped varistors. This result may be a good evidence to confirm the result of *C–V* measurements and above discussions about them. That is, we can see that the concentration of donor defects, $Zn_i^{\bullet}$ or $V_o^{\bullet}$ [20, 22, 23], is reduced by annealing in air and not in inert gases.

Assuming that $n = [Zn_i^{\bullet}]$, the following empirical equation has been obtained [24],

$$n = 3.8 \times 10^2 P_{O_2}^{-1/4} \exp(-2.3e/kT) \quad (9)$$

where P_{O_2} is the oxygen partial pressure. It should be, however, noted that the equally agreeable relationship with the experimental result can be obtained by assuming that oxygen vacancies are the donor species in ZnO, $n = [V_o^{\bullet}]$ [24],

$$n = 3.3 \times 10^2 P_{O_2}^{-1/4} \exp(-2.48e/kT) \quad (10)$$

Both the above two equations show that the donor concentration (= carrier concentration) increases with soaking temperature. Therefore, it can be easily seen that the donor concentration of the as-sintered samples is higher than that of the samples treated at lower temperatures. This means that the varistor samples sintered at 1150° C in air have a higher carrier concentration than the specimens annealed at 750° C in air. However, when annealing is performed in an inert gas atmosphere, the value of P_{O_2} goes to zero and so the carrier concentration remains constant as the sintered state. Therefore, the result in Fig. 5, which shows smaller leakage current in case of the varistors annealed in air, can be explained from the decrease of donor density by the thermal oxidation of the donor species.

On the other hand, the effect of annealing time on the *E–J* characteristics is shown in Fig. 6, from which the grain boundary barrier potential Φ can be presented as a function of annealing time. Equations 9 and 10 are useful in such a case that equilibria between the concentration of donor defects and the oxygen partial pressure are established. However, the reaction of the donor defects with oxygen in air during annealing will be controlled by diffusion processes of the donor species. This means the donor concentration of the

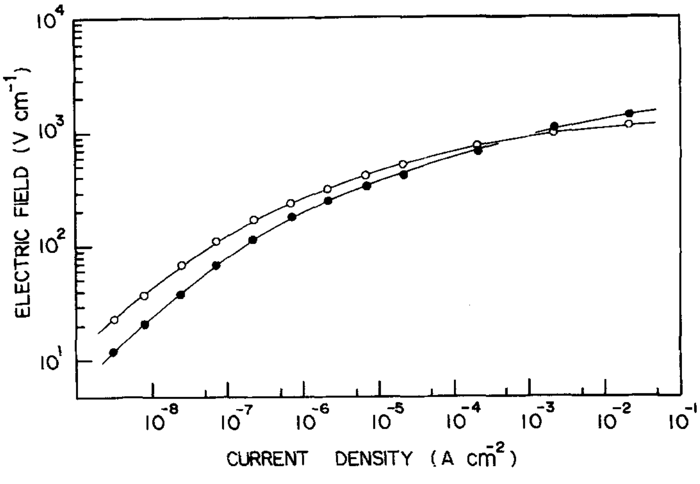

Figure 5 Effect of atmosphere for annealing on the *E–J* characteristics of Co_2O_3-doped composite. (○) in air, (●) in nitrogen; at 750° C for 3 h.

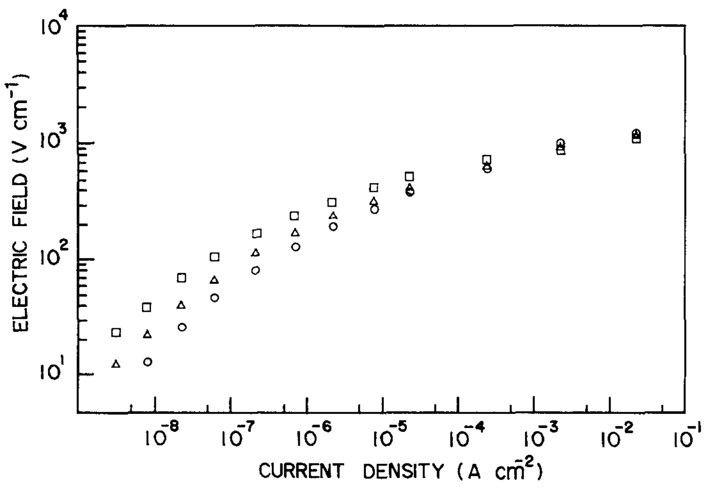

Figure 6 E–J characteristics of the varistor doped with Co_2O_3 as a parameter of annealing time. (○) 0.4 h, (△) 1.0 h, (□) 3.0 h.

varistor samples is reciprocal with annealing time and eventually reaches the equilibrium concentration at 750° C in air, equivalent to Equation 9 or 10.

Consequently, it can be concluded that the gradual recovery of varistor non-linearity with ageing time (in air), resulted from the decrease of leakage current as can be seen in Table I, is probably attributed to the oxidation of the donor species.

Variation of barrier height as a function of annealing time must be also related with fluctuations of N_s during the annealing process because N_s is certainly influenced by the oxidation process besides the transformation of the intergranular phases. However, it is with regret that the variation of N_s with annealing time is not yet studied quantitatively in this work. More intensive studies will be continued in this field and submitted in a coming paper.

4. Summary

Effects of annealing on the potential barrier at the grain boundaries of ZnO varistors were investigated by means of E–J characteristic measurements and analyses of C–V measurements, XRD patterns, and scanning electron micrographs.

The E–J measurements indicated that:

1. Leakage current becomes larger by annealing at 750° C;

2. Annealed samples in nitrogen have a little larger leakage current than those annealed in air;

3. Voltage–current non-linearity of the annealed samples is gradually restored with annealing time (in air), due to the decrease of leakage current which results in smaller power consumption.

From the analysis of C–V characteristics, the following results were obtained:

4. Built-in barrier voltage $\emptyset$ is dramatically lowered by the treatment, while those of the samples treated in air present a little higher than those of the treated in argon;

5. Donor concentration in ZnO grains decreases by annealing in air but little influenced in argon.

XRD patterns and electron micrographs showed that:

6. The phase transition of Bi_2O_3 intergranular layers from α-phase to γ-phase accompanied with a morphological change occurs by annealing at 750° C.

From these experimental results, it can be concluded that:

(i) The grain boundary potential barrier is lowered by annealing at 750° C and this is explained by the lowered built-in voltage attributed to the decrease of surface state density, which may correspond to the phase transformation of Bi_2O_3 intergranular layers.

(ii) The higher non-linearity of the sample annealed in air and the gradual recovery of non-linearity with the increase of annealing (in air) time are responsible for the decrease of the donor density due to the thermal oxidation of Zn_i or V_o in ZnO grains.

References

1. M. MATSUOKA, *Jpn. J. Appl. Phys.* **10** (1971) 763.
2. J. D. LEVINE, *CRC Crit. Rev. Solid State Sci.* **5** (1975) 597.
3. P. R. EMTAGE, *J. Appl. Phys.* **48** (1977) 4372.
4. K. EDA, *ibid.* **49** (1978) 2694.
5. G. D. MAHAN, *ibid.* **54** (1983) 3825.
6. J. BERNASCONI, S. STRASSLER, B. KNECHT, H. P. KLEIN and A. MENTH, *Solid State Commun.* **21** (1977) 867.
7. L. M. LEVINSON and H. R. PHILIPP, *J. Appl. Phys.* **46** (1975) 1332.
8. G. D. MAHAN, L. M. LEVINSON and H. R. PHILIPP, *ibid.* **50** (1979) 2799.
9. L. M. LEVINSON and H. R. PHILIPP, *ibid.* **47** (1976) 3116.
10. A. IGA, M. MATSUOKA and T. MASUYAMA, *Jpn. J. Appl. Phys.* **15** (1976) 1161.
11. N. SHOHATA and J. YOSHIDA, *ibid.* **16** (1977) 2299.
12. A. IGA, M. MATSUOKA and T. MASUYAMA, *ibid.* **15** (1976) 1847.
13. M. INADA, *ibid.* **18** (1979) 1439.
14. T. TAKAWAGUCHI, H. YOSHIDA and M. KAWAI, *J. Electron. Photograph.* **7** (1966) 24.
15. K. EDA, A. IGA and M. MATSUOKA, *J. Appl. Phys.* **51** (1980) 2678.
16. M. MATSUOKA, in "Advances in Ceramics", Vol. 1, edited by L. M. Levinson and D. C. Hill (American Ceramic Society, Columbus, 1981) p. 190.
17. M. H. OH, Korea Institute of Science and Technology Research Report, BS E508 (5)-1479-4 (December, 1980).
18. E. SONDER and W. G. AUSTIN, *J. Appl. Phys.* **54** (1983) 3566.

19. W. G. MORRIS, *J. Vac. Sci. Technol.* **13** (1976) 926.
20. W. D. KINGERY, H. K. BOWEN and D. R. UHLMANN, in "Introduction to Ceramics" (Wiley, New York, 1976) Chs 4 and 9.
21. J. WONG and W. G. MORRIS, *Ceram. Bull.* **53** (1974) 916.
22. R. H. SWALIN, in "Thermodynamics of Solids" (Wiley, New York, 1972) Ch. 14.
23. S. SHIRASAKI, *Ceramics (Jpn)* **18** (1983) 918.
24. Z. M. JARZEBSKI, in "Oxide Semiconductors", 1st English Edn (Pergamon Press, Oxford, 1973), Ch. 13.2.

Received 11 April
and accepted 4 December 1985